OPEN

npg

The p38α mitogen-activated protein kinase is a key regulator of myelination and remyelination in the CNS

S-H Chung[*,1,2], S Biswas[1], V Selvaraj[1,3], X-B Liu[1], J Sohn[4], P Jiang[1], C Chen[1], F Chmilewsky[2], H Marzban[5], M Horiuchi[4], DE Pleasure[4] and W Deng[*,1,4,6]

The p38α mitogen-activated protein kinase (MAPK) is one of the serine/threonine kinases regulating a variety of biological processes, including cell-type specification, differentiation and migration. Previous *in vitro* studies using pharmacological inhibitors suggested that p38 MAPK is essential for oligodendrocyte (OL) differentiation and myelination. To investigate the specific roles of p38α MAPK in OL development and myelination *in vivo*, we generated p38α conditional knockout (CKO) mice under the PLP and nerve/glial antigen 2 (NG2) gene promoters, as these genes are specifically expressed in OL progenitor cells (OPCs). Our data revealed that myelin synthesis was completely inhibited in OLs differentiated from primary OPC cultures derived from the NG2 Cre-p38α CKO mouse brains. Although an *in vivo* myelination defect was not obvious after gross examination of these mice, electron microscopic analysis showed that the ultrastructure of myelin bundles was severely impaired. Moreover, the onset of myelination in the corpus callosum was delayed in the knockout mice compared with p38α fl/fl control mice. A delay in OL differentiation in the central nervous system was observed with concomitant downregulation in the expression of OPC- and OL-specific genes such as Olig1 and Zfp488 during early postnatal development. OPC proliferation was not affected during this time. These data indicate that p38α is a positive regulator of OL differentiation and myelination. Unexpectedly, we observed an opposite effect of p38α on remyelination in the cuprizone-induced demyelination model. The p38α CKO mice exhibited better remyelination capability compared with p38α fl/fl mice following demyelination. The opposing roles of p38α in myelination and remyelination could be due to a strong anti-inflammatory effect of p38α or a dual reciprocal regulatory action of p38α on myelin formation during development and on remyelination after demyelination.
Cell Death and Disease (2015) 6, e1748; doi:10.1038/cddis.2015.119; published online 7 May 2015

The myelin sheath is the fatty insulating layer that wraps around the axons of the nerves and is critical to the efficient conduction of nerve impulses. It is produced by a specialized glial cell called oligodendrocyte (OL) in the central nervous system (CNS). The proper development of OL and myelination is essential for maintaining the efficiency and speed of electrical nerve impulse. The damage to the developing OL and myelin is a hallmark of many demyelinating and dysmyelinating disorders, including the autoimmune disorders such as multiple sclerosis (MS) as well as periventricular leukomalacia, which is the predominate form of white matter injury seen in premature infants, leading to disability and neurological and cognitive impairments.[1–3]

Myelination is a complicated process involving generation of OL progenitor cells (OPCs), differentiation of OPCs into myelinating OLs, ensheathment of axons by OLs and finally

wrapping the nerves with the expansion of myelin sheath.[4–6] The study of intracellular signals that regulate myelinogenesis is crucial to our understanding of the developmental and pathological processes in white matter structures.

The mitogen-activated protein kinases (MAPKs) belong to the family of serine/threonine protein kinases that allow cells to respond to stimuli received from their extracellular environment, including mitogens as well as to intracellular stress. The p38 MAPK family members (p38α, p38β, p38γ and p38δ) in particular are implicated in various biological processes, such as cell survival, proliferation and differentiation.[7–10] The p38α is well established as a mediator of stress responses in neural cells; however, its physiological role(s) during OL development and myelination has only been recognized recently.[11–16] Using p38 inhibitors, several studies have demonstrated that p38α MAPK is important for myelination in cultured Schwann cells[11]

and OPCs.[12] In addition, p38α has been reported to affect both cell proliferation and glial lineage progression in the presence of growth factors.[17] More recently, Hossain *et al*.[15] demonstrated that p38α controls Krox-20 to regulate Schwann cell differentiation and peripheral myelination. In contrast, p38 has also been reported as a negative regulator of Schwann cell differentiation and myelination.[16] However, most studies were carried out using *in vitro* glial cell culture systems and with p38 inhibitors that were not selective for the p38α isoform. The *in vivo* molecular mechanisms and signaling events by which p38α regulates OPC development and myelination, therefore, remain elusive.

In an effort to identify the specific role(s) of p38α in myelination during early postnatal development, we have bred p38α-floxed (p38α fl/fl) mice with nerve/glial antigen 2 (NG2) or proteolipid peptide (PLP)-cre mice to generate homozygous conditional NG2/Plp-specific p38α knockout mice for the first time. Our data showed that p38 *α* is a positive regulator of OL development and myelination during CNS development as both myelination and OL development were impaired in specific forebrain regions of the conditional knockout (CKO) mice. Surprisingly, we observed an opposite effect of p38α on remyelination in the cuprizone-induced demyelination model. Our findings identified novel reciprocal roles of p38α during OL development in the early postnatal brain and during remyelination in adult mice, implicating the therapeutic potential of p38α inhibition in CNS remyelination.

Results

Generation of OPC-specific p38α knockout mice. To identify the specific *in vivo* role(s) of p38α in OL development and myelination, we have generated two conditional OPC-specific p38α knockout mice by crossing NG2-Cre or plp-Cre mice with p38α-floxed (p38α fl/fl) mice.[18] The targeted disruption of the p38α gene in NG2^{cre}/p38α$^{-/-}$ or Plp^{cre}p38α$^{-/-}$ (p38α CKO) mice was mediated by Cre-loxP recombination under the control of the NG2 or the Plp promoter. The p38α gene deletion only occurred in specific cell types with an active NG2 or Plp promoter as illustrated (Figure 1a). We also utilized a reporter strain (EYFP and ROSA26-mT/mG) to simultaneously validate Cre recombination in these cells (Figures 1b and c). The genotype of NG2-Cre p38α CKO mice was confirmed by the presence of homozygous p38a-floxed alleles and being positive for NG2-Cre transgene (Figure 1d). The p38α CKO mice were viable with no obvious abnormalities at the gross phenotypic level.

***In vitro* myelination is blocked in the NG2 p38α CKO-derived OLs.** We first examined whether endogenous p38α deletion in OPCs affected their ability to form myelin after differentiation *in vitro*. To achieve this, we first generated OPC cultures using pups from cross breed of homozygous ROSA26-tdTomato-EGFP (enhanced green fluorescent protein) and NG2-Cre mice, in which, tdTomato gene is excised by Cre recombinase, leading to EGFP expression in cells with a constitutive NG2 promoter (Figures 1e and g). After OL cultures were made from p38afl/fl and NG2-Cre p38α mice, we confirmed for the absence of p38a protein expression in

cultures (Figure 1d). Purified OPCs from p38α CKO and p38α fl/fl mice were differentiated *in vitro* for 4 days (Figures 1e and g). Consistent with the previous studies,[11,12] the expression of myelin basic protein (MBP), a major protein of central and peripheral myelin, was completely diminished in the p38α CKO OLs (green cells in Figures 1i and l), whereas p38α fl/fl OLs expressed MBP (red cells in Figures 1j and l). This result further confirmed a critical role of p38α in normal myelin production at least *in vitro*.

Myelination defects in p38α CKO mice. We next sought to investigate the extent of *in vivo* myelination in the neonatal p38α CKO mice. Surprisingly, under the light microscope, dense and compact MBP staining was seen throughout the white matter regions of the p38α CKO brain. Although the MBP staining intensity in some areas of the corpus callosum (CC) tended to be weaker in the CKO compared with p38α fl/fl, the differences in general were not significant at low magnification (Figure 2). The mean MBP staining intensity was $78.1 \pm 5\%$ (compared with same regions in p38α fl/fl assigned as 100%, analyzed from 117 different observation fields, $N = 12$, $P = 0.008$) in the CC and $87.5 \pm 11\%$ (analyzed from 83 different observation fields, $N = 7$, $P = 0.449$) in the striatum (St) compared with the p38α fl/fl mouse brains. Western blotting analysis of the whole brain between the p38α CKO and p38α fl/fl did not show any noticeable difference in the MBP expression (Figure 2i).

However, a detailed morphological observation using electron microscopy revealed several characteristic myelination and axonal defects in the p38α CKO brain. We observed axonal swellings (Figure 3b: arrows), changes in the axon density (Figures 3c and d) and axon degeneration (Figure 3e) at postnatal day (P) 12. These morphological changes that were indicative of degenerating axons suggest that p38α has an important role in establishing complete and functional axons. In p38α CKO, the thickness of the myelin sheath surrounding the axons was significantly reduced compared with p38α fl/fl mice (Figures 3j and l). Myelin thickness was measured as the g-ratio (the ratio of axon diameter to fiber diameter). A total of 380 axons from 7 mice were investigated from different non-overlapping observational fields (OF). The average thickness of axons from p38α CKO mice was $2.91 \pm 0.07\,\mu m$ (348 OF, $N = 8$, $P < 0.0001$ compared with p38α fl/fl), while axons from p38α fl/fl mice were typically $3.73 \pm 0.14\,\mu m$ thick (126 OF, $N = 6$). The average *g*-ratio of the nerve fibers from p38α CKO mice was 0.818 ± 0.01 (276 OF, $N = 8$) compared with 0.693 ± 0.02 (234 OF, $N = 6$) in p38α fl/fl mice, thus suggesting a significant thinner myelin sheath in p38α CKO ($P < 0.0001$ compared with p38α fl/fl). The myelination defect phenotype is mainly observed in early stage of myelination, and the phenotype is less obvious in adult/old p38α CKO mice. The average thickness of axons from P90 p38α CKO mice was $4.59 \pm 0.63\,\mu m$ (87 OF, $N = 3$, $P < 0.0001$ compared with p38α fl/fl), while axons from p38α fl/fl mice were typically $5.27 \pm 0.54\,\mu m$ thick (43 OF, $N = 2$).

P38α CKO results in a delay in the onset of myelination in the CC. As we observed that the ultrastructural myelination defects in the p38α CKO were more pronounced in early stages of myelination, we studied the myelination pattern at
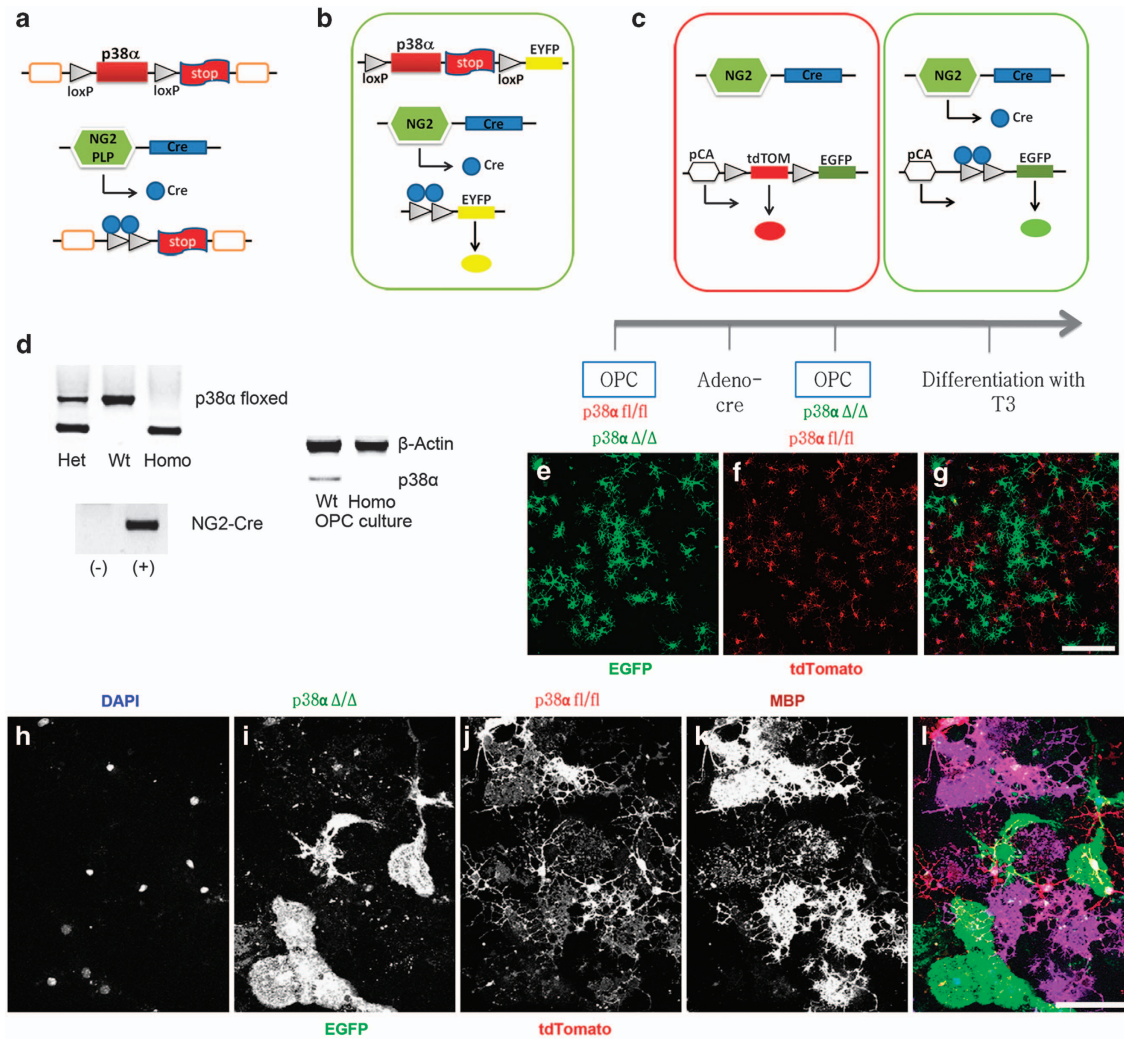
Figure 1 Generation of NG2/Plp^{Cre}p38α CKO mice and *in vitro* differentiation of p38α CKO OPCs. (**a**) Generation of p38α CKO mice by crossing NG2/Plp-Cre mice and mice with p38α-floxed alleles (p38α fl/fl). Schematic diagram showing the targeted genetic locus of p38α gene flanked by two loxP sites. p38α gene deletion is driven by Cre-loxP recombination that is under the control of NG2/Plp promoter activity in targeted cells. (**b** and **c**) Schematic illustrations demonstrating the EYFP (**b**) and ROSA26tdTomato (**c**) reporter system. Under the control of NG2/Plp promoter, Cre recombination results in an excision of tdTomato (mT) and the expression of EGFP (mG) in NG2/Plp-positive cells. (**d**) Genotyping of NG2-Cre mice demonstrating homozygosity of p38α-floxed allele and positive expression of NG2-Cre transgene. Western blotting analysis confirmed that the p38a protein is absent in p38α CKO OPC cultures. (**e**–**g**) Schematic diagram of *in vitro* differentiation of purified primary OPCs from CKO mice. Four days after culture, both p38α CKO (green: **e**) and p38α fl/fl cells (red: **f**) were observed. (**h**–**l**) Immunohistochemistry for anti-MBP after terminal differentiation of OPCs into myelin-forming OLs. MBP immunofluorescence labeling demonstrates that MBP expression was diminished in p38α CKO cells (green cells in panels (**i**) and (**l**)), while p38α fl/fl cells express MBP (red cells in panels (**j**) and (**l**)). Scale bars: panel (**g**) = 500 μm; panel (**l**) = 50 μm

several early embryonic developmental stages. To identify a myelination phenotype during development in the p38α CKO, we directly compared the intensity and pattern of MBP staining in brain sections from P5, P7 and P12 from p38α CKO and p38α fl/fl control mice. In P5 p38α fl/fl brains, strong MBP immunostaining was seen in the CC, as expected (Figure 4a). In contrast, the intensity of MBP immunostaining in the CC was significantly weaker in the p38α CKO (Figure 4d). In the p38α CKO St, onset of myelination was observed (Figure 4a), while onset of myelination had not taken place in most areas of the St in p38α fl/fl (Figure 4d). At P7, the MBP-positive band in the CC was found to be thinner in p38α CKO mice (Figures 4e and h) compared with p38α fl/fl control (Figures 4b and g). In addition, the intensity of MBP staining in the CC was significantly less in the p38α CKO CC

(Figures 4e and h) compared with p38α fl/fl (Figures 4b and g). However, at P12, the intensity of MBP staining in the CC between the p38α fl/fl and p38α CKO brain became comparable (Figures 4c and f). The fluorescence intensity of MBP staining in the CC was quantified in numerous non-overlapping OF (Figure 4i). The fluorescence intensity of MBP staining at P5 was $24.9 \pm 6.2\%$ (237 OF, $N = 13$, $P < 0.0001$), at P7 $37.2 \pm 7.5\%$ (177 OF, $N = 9$, $P < 0.0001$) and at P12 $82.9 \pm 13\%$ (274 OF, $N = 17$, $P = 0.23$), compared with p38α fl/fl control (521 OF, $N = 34$, assigned as 100%). Next we investigated whether these myelination defects are the direct result of knocking out p38α from cells. The EYFP reporter system allows us to visualize the cells when the p38α gene is excised out and Cre is expressed in the cells.
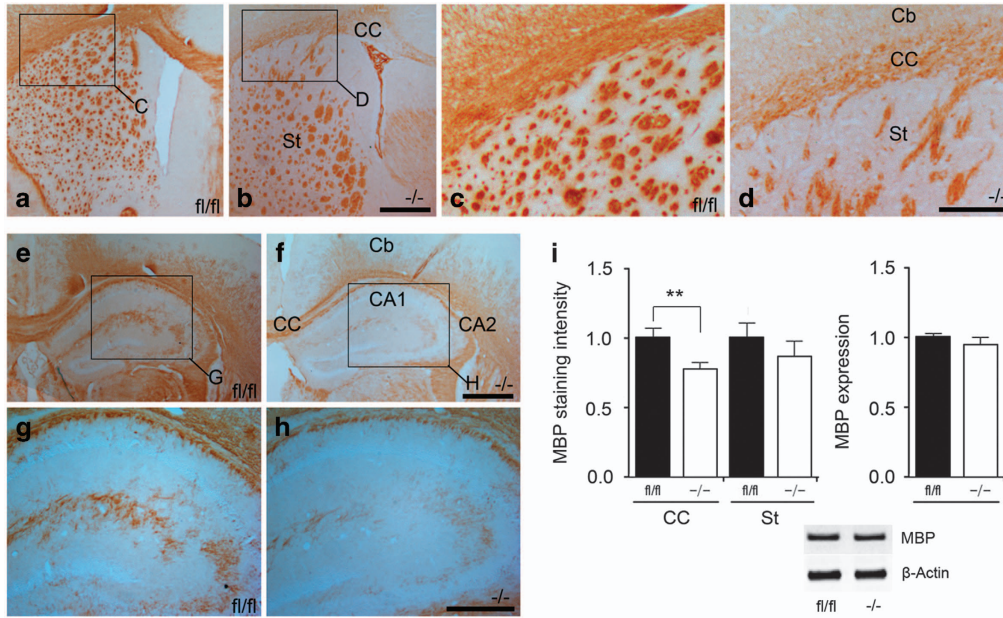
Figure 2 No obvious gross myelination defects were observed in p38α CKO mice. (**a–d**) Transverse sections were peroxidase stained for anti-MBP in p38α fl/fl (**a** and **c**) and p38α CKO (**b** and **d**) at P28. Panels (**c**) and (**d**) are higher magnification views of the regions indicated in panels (**a**) and (**b**). (**e–h**) Transverse sections peroxidase stained for anti-MBP in p38α fl/fl (**e** and **g**) and p38α CKO (**f** and **h**) at P28. Panels (**g**) and (**h**) are higher magnification views of the regions indicated in panels (**e**) and (**f**). MBP expression in some areas of the CC seemed to be relatively weak in the knockout compared with p38α fl/fl, but generally the difference was not obvious at low magnification of light microscope level. (**i**) Statistical analysis of the MBP staining intensity in the CC ($P < 0.01$) and St of P28 p38α CKO and p38α fl/fl mice. Western blotting analysis of MBP protein in the whole brains of P28 p38α CKO and p38α fl/fl mice. **$P < 0.01$. Abbreviation: Cb, cerebral cortex. Scale bars: panel (**b**) = 500 μm; panel (**d**) = 250 μm; panel (**f**) = 500 μm; panel (**h**) = 250 μm

Immunostained sections of p38α CKO CC using anti-EYFP (green) and anti-MBP antibodies (red) showed that the onset and progression of myelination are delayed at different developmental stages (Figures 4j and o). The green cells (p38α knockout cells) generally did not overlap with the MBP staining (red), suggesting that knockout cells produced none or negligible myelin compared with p38α fl/fl cells at similar developmental stages of myelination (Figures 4j, o and 5).

OPC differentiation is delayed in p38α CKO. We then assessed whether the deletion of p38α gene affects the proliferation of OPCs that in turn would lead to myelination defects in the p38α CKO mice. The numbers of Olig2-positive cells in the CC of p38α fl/fl and p38α CKO mice were examined at P0 and P7. Olig2-positive OPC numbers were unchanged in the p38α CKO at both time points (Figures 6a and c). Quantitatively, at P0, the numbers of Olig2-positive cells were 168 ± 14 in p38α fl/fl (223 areas were examined, $N = 8$) versus 154 ± 47 in p38α CKO (276 areas were examined, $N = 12$, $P = 0.81$); and at P7 the numbers of Olig2-positive cells were 237 ± 12 in p38α fl/fl (186 areas were examined, $N = 8$) versus 257 ± 13 in p38α CKO (263 areas were examined, $N = 11$, $P = 0.31$). These results suggested that p38α did not have a role in OPC proliferation during perinatal and postnatal development.

We next examined the effects of p38α deletion on the expression of various stage specific OPC and OL mRNAs, including Brg1, Olig1, Olig2, Zfp488 and NG2, using qPCR analysis. It has been recently shown that Smarca4/Brg1 is necessary and sufficient to initiate and promote OL lineage progression and maturation.[16] Basic helix-loop-helix

transcription factors Olig1 and Olig2 have been shown to regulate OL development.[19,20] Zfp488 is an OL-specific zinc finger protein, identified as a downstream effector of Olig1, which physically cooperates with Olig2 during OL differentiation.[21–23] NG2 is a chondroitin sulfate proteoglycan and NG2+ cells have been recognized as OPCs. Our qPCR expression results showed at P0 there was significantly reduced expression of Brg1 ($100 \pm 11\%$ in p38α fl/fl versus $71.2 \pm 14\%$ in p38α CKO, $P = 0.039$), Olig1 ($100 \pm 7.6\%$ in p38α fl/fl versus $44.3 \pm 6.2\%$ in p38α CKO, $P < 0.0001$), Zfp488 ($100 \pm 32\%$ in p38α fl/fl versus $8.21 \pm 7.8\%$ in p38α CKO, $P = 0.013$) and NG2 ($100 \pm 11\%$ in p38α fl/fl versus $65.2 \pm 13\%$ in p38α CKO, $P = 0.048$) mRNAs (Figures 6d and h). However, downregulation of Olig1, Zfp488 and NG2 expression in the p38α CKO was restricted to an early stage of OPC differentiation (P0). By P7, the expression levels of the following genes were comparable between the p38α fl/fl and CKO mice: Olig1, $15.6 \pm 6.1\%$ in p38α fl/fl versus $10.2 \pm 0.6\%$ in p38α CKO, $P = 0.391$; Zfp488 $11.5 \pm 0.69\%$ in p38α fl/fl versus $10.3 \pm 0.2\%$ in p38α CKO, $P = 0.113$; and NG2, $56.2 \pm 18\%$ in p38α fl/fl versus $42.6 \pm 20\%$ in p38α CKO, $P = 0.625$. Olig2 expression was not significantly different between the p38α CKO and p38α fl/fl both at P0 and P7 (Figure 6h). These results suggest that p38α gene deletion affected OPC differentiation without affecting proliferation, and this, in turn, might contribute to a delayed onset of the myelination.

p38α CKO promotes remyelination after cuprizone-induced demyelination. We next examined the specific role of p38α isoform in the cuprizone-induced demyelination/remyelination model. Mice that were on cuprizone diet for
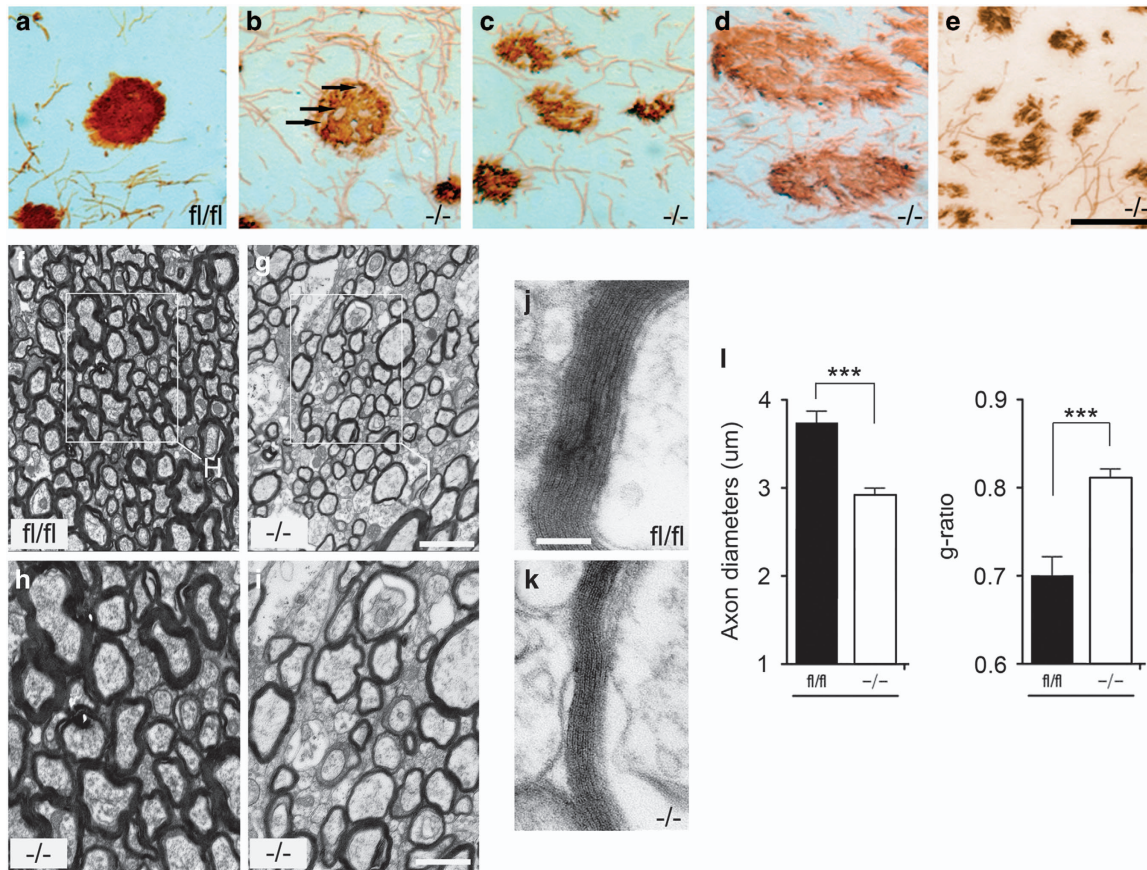
Figure 3 p38α CKO mice show morphological defects and reduced axon diameters. (**a–e**) Sagittal sections were peroxidase stained for anti-MBP in p38α fl/fl (**a**) and p38α CKO (**b–d**) at P12. Axonopathies observed in the p38α CKO: axonal swelling (**b** and **c**), changes in the density of axons (**c** and **d**) and degeneration (**e**) were frequently seen. (**f–k**) Electron microscopic analysis of myelinated bundles in CC sections from P12 p38α CKO and p38α fl/fl mice. Panels (**h**) and (**i**) are higher magnification views of the regions indicated in panels (**f**) and (**g**). The thickness of myelin bundle diameter surrounding the axons was significantly reduced in the p38α CKO (**k**) compared with p38α fl/fl (**j**). (**h**) and (**i**) are higher magnification views of the regions indicated in panels (**f**) and (**g**). (**l**) Quantification of axon diameters and *g*-ratio (the ratio of axon diameter to fiber diameter). The axon diameters were significantly reduced in the CKO CC ($P < 0.0001$). The *g*-ratio was significantly increased from 0.693 in p38α fl/fl to 0.818 in p38α CKO mice ($P < 0.0001$). ***$P < 0.005$. Scale bars: panel (**e**) = 50 μm; panel (**g**) = 5 μm; panel (**h**) = 2.5 μm; panel (**j**) = 1 μm

5 weeks progressively lost myelin as indicated by the loss of MBP immunostaining in the CC. When mice were returned to normal diet, immediate remyelination and recovery process began. To identify the remyelination phenotype, a peroxidase immunohistochemistry with anti-MBP antibody was performed. Unexpectedly, we observed a reverse effect of p38α on remyelination in cuprizone-induced demyelination model. The p38α CKO mice showed better remyelination ability than the p38α fl/fl mice (Figure 7). The intensity of MBP staining was similar after 1 week of recovery between the p38α fl/fl ($100 \pm 12\%$) (223 different areas were examined, $N = 16$) and p38α CKO brains ($91 \pm 8.0\%$) (178 different areas were examined, $N = 13$, $P = 0.565$) and also, after 2 weeks, $100 \pm 7.3\%$ in p38α fl/fl (198 different areas were examined, $N = 14$) *versus* $106 \pm 6.1\%$ in p38α CKO (246 different areas were examined, $N = 17$, $P = 0.530$). However the remyelination ability was significantly increased in p38α CKO mice after the third week of recovery. MBP staining intensity in p38α fl/fl was $100 \pm 4.4\%$ (179 different areas were examined, $N = 12$) *versus* $134 \pm 13\%$ in p38α CKO (231 different areas were examined, $N = 14$, $P = 0.030$). In addition, the thickness of MBP-stained axon bundles in the p38α

CKO CC was increased 1.32-fold ($132 \pm 12\%$) (215 different areas were examined 215, $N = 16$) compared with the p38α fl/fl control ($100 \pm 6.2\%$, 193 different areas were examined 193, $N = 15$, $P = 0.031$).

Discussion

In this study, we report the specific *in vivo* role of the p38α MAPK isoform in myelin formation during development, as well as during remyelination, for the first time, by generating OL-specific p38α CKO mice. Our main finding was that, although a myelination phenotype was not evident at a gross level, there were several myelination defects at the ultra-structural level. Specifically, myelin bundles in the CC failed to develop normally, and there was a delayed onset of myelination in the CC. These defects could be partly due to a delay in OL differentiation during postnatal development as OPC proliferation remained normal in these knockout mice. This was supported by our observation that gene expression levels of several critical transcription factors of OPC maturation such as Olig1, Zfp488, and the OPC marker NG2 were significantly downregulated during early neonatal development in these
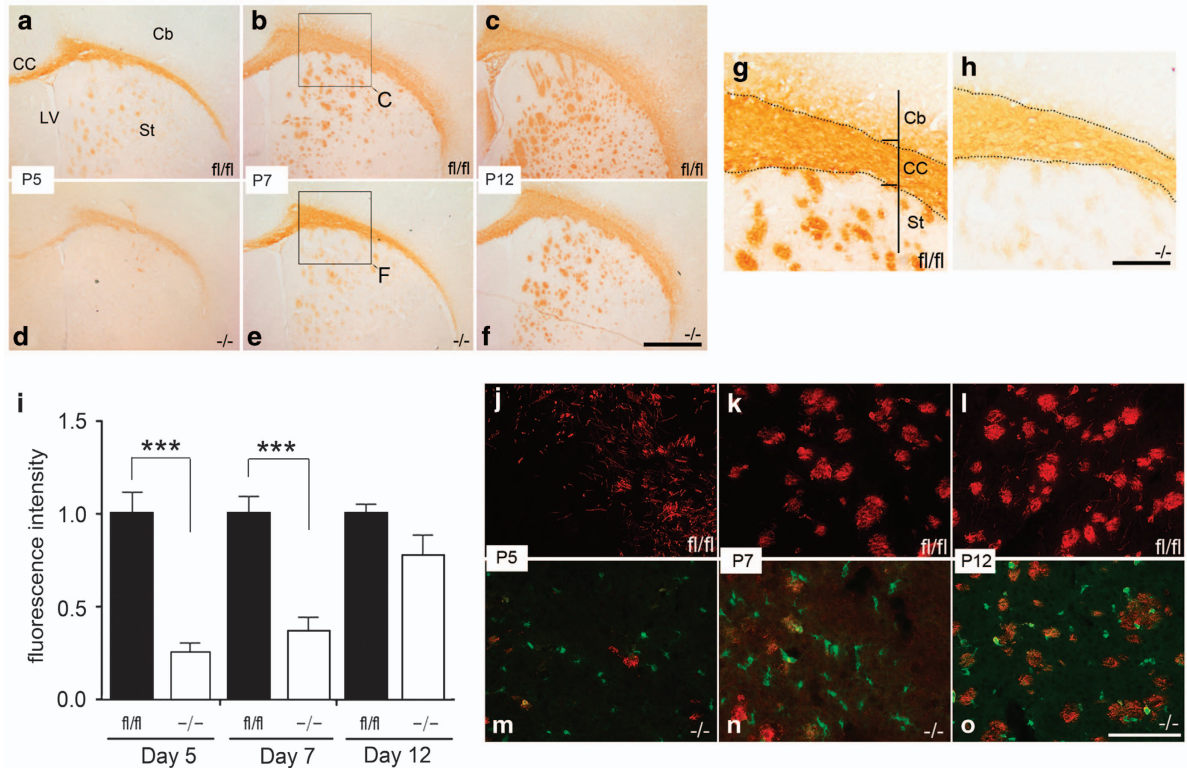
Figure 4 Delay in the onset of myelination in the CC of p38α CKO mice. (**a–h**) Transverse sections peroxidase stained for anti-MBP at P5, P7 and P12 in p38α fl/fl and p38α CKO revealed that the onset and progression of myelination were delayed in the p38α CKO. Panels (**g**) and (**h**) are higher magnification views of the regions indicated in panels (**b**) and (**e**). (**i**) Quantitative analysis of MBP expression during different postnatal periods in the CC of the p38α fl/fl and p38α CKO mice, suggesting a delay in onset of myelination (P5 and P7 $P < 0.0001$). (**j–o**) Immunofluorescence-stained sections with anti-EYFP (green) and MBP (red) showed that the onset and progression of myelination were delayed in the p38α CKO CC. Green cells represent p38α knockout cells. Abbreviations: Cb, cerebral cortex; LV, lateral ventricle. ***$P < 0.005$. Scale bars: panel (**f**) = 250 μm; panel (**h**) = 75 μm; panel (**o**) = 250 μm
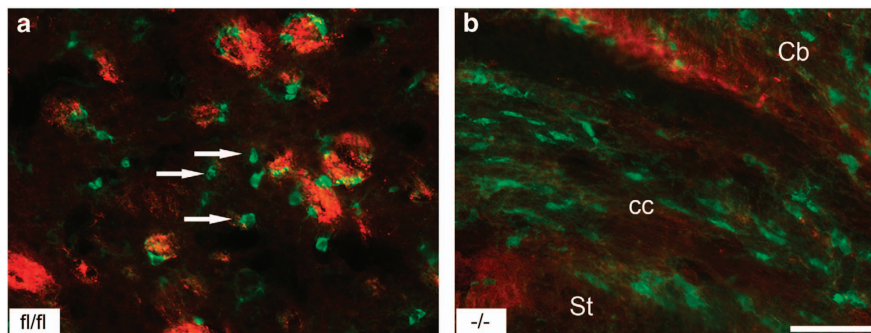

Figure 5 The p38α knockout cells show myelination defects *in vivo*. Immunofluorescence-stained sections with anti-EYFP (green) and MBP (red) in the (**a**) St and (**b**) CC of p38α CKO mice. Green cells represent p38α knockout cells. Majority of p38α knockout cells (arrows) did not express MBP. Abbreviation: Cb, cerebral cortex. Scale bar: panel (**b**) = 100 μm

knockout mice. Additionally, similar to previous reports, an inherent myelination defect was apparent in the primary OPCs isolated from p38α CKO mouse brains. These OPCs failed to synthesize MBP when differentiated *in vitro*. Our second major finding was that p38α appears to have a negative regulatory role during remyelination in cuprizone-induced demyelination model in adult p38α CKO mice. The p38α CKO mice showed enhanced remyelination ability compared with p38α fl/fl during the recovery period.

Understanding the intracellular signals that regulate myelination during development or following demyelination is crucial for identifying developmental and pathological processes in several dysmyelinating disorders, including leukodystrophies, and demyelinating disorders, such as MS. The p38 MAPK signaling pathway has been initially shown to be activated by stress stimuli and to induce inflammatory responses.[7–10] Recent studies have recognized its critical role in myelination but mostly in the peripheral nervous system.
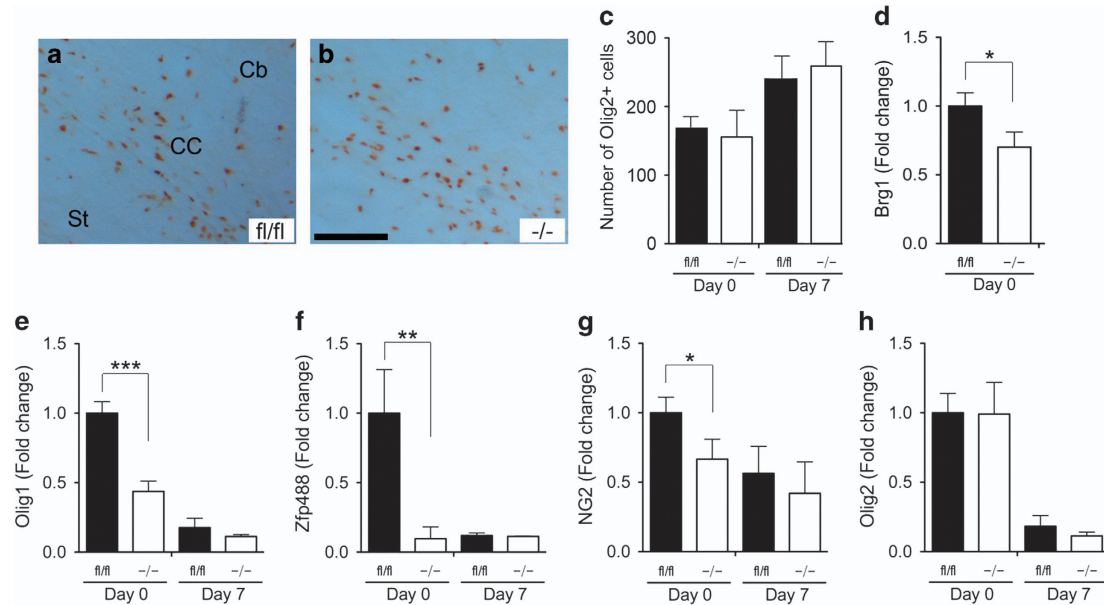
Figure 6 p38α gene deletion results in a delayed OL differentiation without affecting proliferation. (**a** and **b**) Transverse sections were peroxidase stained for anti-Olig2 at P7 in the CC of the p38α fl/fl (**a**) and p38α CKO mice (**b**). (**c**) Quantification of Olig2-immunopositive cells in the CC at P0 and P3 in the p38α fl/fl and p38α CKO. The numbers of Olig2-posivtive cells were unchanged. (**d**–**h**) Quantitative PCR analysis for Brg1 (**d**), Olig1 (**e**), Zfp488 (**f**), NG2 (**g**) and olig2 (**h**) at P0 and P7 in the p38α fl/fl and p38α CKO mice. Olig1 and Zfp488 expression is significantly downregulated in the P0 p38α CKO mice (**e** and **f**). $*P < 0.05$, $**P < 0.01$ $***P < 0.005$. Abbreviation: Cb, cerebral cortex. Scale bar: panel (**b**) = 100 μm

Initially, Fragoso *et al.*[11] showed that p38 inhibition by p38 MAPK pharmacological agents blocks myelin formation in cultured Schwann cells. Forskolin-induced MBP gene expression was also blocked by the p38 inhibitor SB203580.[13] Hossain *et al.*[15] demonstrated that p38α MAPK controls Krox-20 to govern Schwann cell differentiation and peripheral myelination. In addition, inhibition of p38 with PD169316 and SB203580 blocked accumulation of protein and mRNA of several cell-stage-specific markers characteristic of differentiated OLs, including MBP.[12] Recently, Cui *et al.*[24] showed that sphingosine 1-phosphate receptor modulates human OL differentiation by activating ERK1/2 and p38 MAPK signaling. These previous studies support p38 MAPK as a positive regulator of OL differentiation and myelination. However, SB203580, the most widely used p38 MAPK inhibitor, is not p38α specific as it blocks both p38α and p38β isoforms and has been reported to target additional proteins, albeit at higher concentrations.[25,26] There is a report showing that p38α and p38γ appear to have opposite functions in skeletal muscle differentiation. p38α has been shown to be a strong promoter of skeletal muscle differentiation, whereas p38γ may act as a negative regulator.[27] Thus the use of nonspecific inhibitors has limitations in revealing a specific role of individual p38 MAPK isoforms. To our knowledge, our study is the first report aimed at identifying a specific *in vivo* role of p38α in OL development and myelination in the CNS.

Our observations with the primary OPC from p38α CKO mice is consistent with the previous studies which demonstrated that myelination was completely inhibited in primary OPC culture from the p38α CKO mice.[12] However, the gross *in vivo* p38α CKO myelin phenotype was not very discernable compared with p38α fl/fl mouse brains. This discrepancy might

be due to the redundant roles of other isoforms of p38 MAPK (p38β, p38γ and p38δ). For example, the two isoforms, p38α and p38β are ~70% identical in their amino-acid sequence, show similar substrate specificity and demonstrate overlapping functions that are critical during mouse embryonic development.

The underlying mechanism of how p38α controls OL differentiation and myelination has not been fully elucidated. Weider *et al.*[28] initially identified an ATP-dependent SWI/SNF chromatin-remodeling enzyme Smarca4/Brg1 to be required for Schwann cell differentiation and myelination. Recently, Yang *et al.*[16] identified that Smarca4/Brg1 is necessary and sufficient to initiate and promote OL lineage progression and maturation. They identified Olig2 as a prepatterning factor that directs the recruitment of Brg1 to OL lineage-specific *cis*-regulatory elements during the critical transition from OPCs to OLs. Our analysis shows that Brg1 is significantly reduced in the p38α CKO cells at P0. Interestingly, in myogenic cell differentiation, p38MAPK appears to regulate Brg1 expression and governs myogenin expression, which has the ability to convert some of the non-muscle cells into the myogenic lineage. Supporting this idea, Li *et al.*[29] found that the p38 MAPK is required for BRG1 recruitment in 12-*O*-tetradeca-noylphorbol-13-acetate-mediated myogenin induction. Thus we speculate that p38α directly regulates Brg1 at early stages of OPC differentiation and myelination. Further studies are warranted to identify the underlying mechanisms by which p38α controls Brg1 in OL differentiation.

An unexpected role of p38α in remyelination was observed in cuprizone-induced demyelination in adult mice. In this model, p38α deletion in OPCs caused hypermyelination following demyelination, as evident by increased thickness
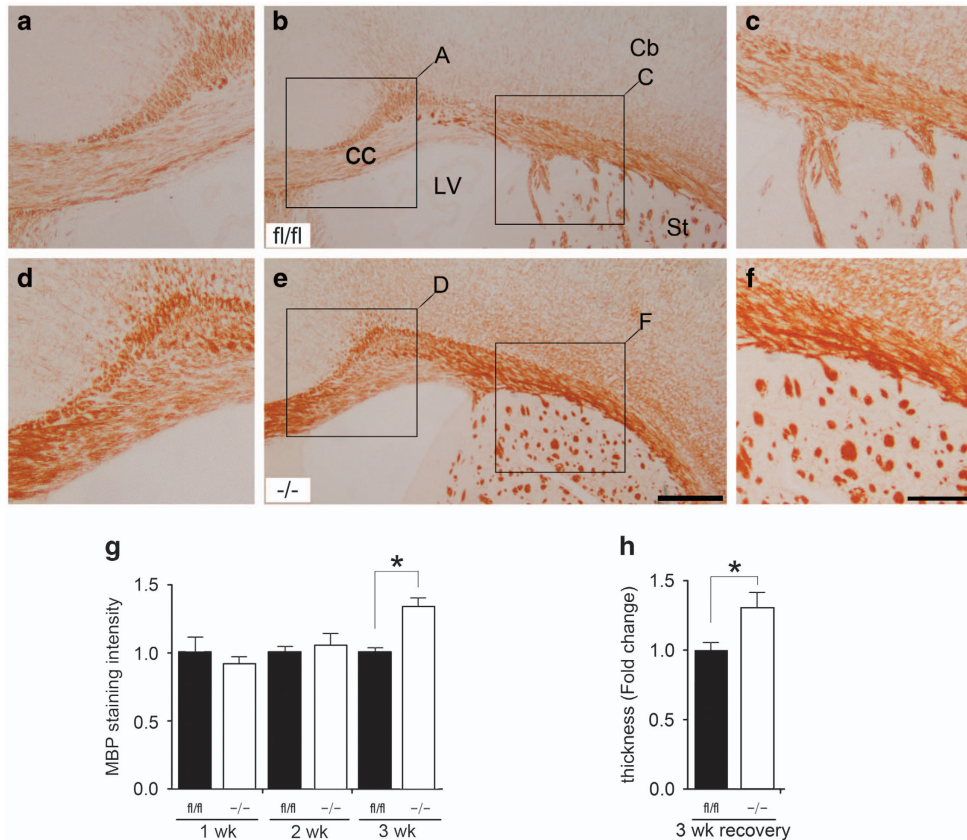
Figure 7 p38α CKO promotes remyelination after cuprizone-induced demyelination. (**a–f**) Transverse sections peroxidase stained with anti-MBP showing remyelination process in the Cc after 3 weeks following discontinuation of cuprizone intake in the p38α fl/fl (**a–c**) and p38α CKO (**d–f**) mice. Panels (**a** and **c**) and (**d** and **f**) are higher magnification views of the regions indicated in panels (**b**) and (**e**), respectively. MBP expression is significantly increased in the CC of p38α CKO (**d–f**) compared with p38α fl/fl (**a–c**) mice. (**g** and **h**) Quantification of MBP staining intensity (**g**) and thickness (**h**) during a recovery period in the p38α fl/fl and p38α CKO. p38α CKO mice showed a better remyelination ability compared with p38α fl/fl during the remyelination process. *$P < 0.05$. Abbreviations: Cb, cerebral cortex; LV, lateral ventricle. Scale bar: panel (**e**) = 500 μm; panel (**f**) = 250 μm

of MBP-stained axon bundles compared with p38α fl/fl control. This suggests that p38α may have a tonic negative regulatory role controlling myelin arrest in adult mice. Overall, our study suggests that p38α could have a dual role as regulator of myelination: during development it acts as a pro-differentiation factor, and but in the adult's brain it participates in myelin arrest. Another possible cause for increased myelination in p38α mice could be due to the anti-inflammatory effect resulting from deletion of p38α. Consequently, p38α could be an interesting pharmaceutical target because of its critical role in inflammatory diseases, such as psoriasis and arthritis. There is an extensive evidence that the p38 MAPK signaling pathway contributes to the proinflammatory cytokine overproduction in many disease states. Cytokine overproduction may contribute towards many neurodegenerative disorders.[30] Supporting this, there is a report that a p38α-specific inhibitor, UR-5269, may have therapeutic role in a widely used mouse model of the MS, experimental autoimmune encephalomyelitis.[31] Several human clinical trials for diseases such as rheumatoid arthritis, asthma, atherosclerosis and acute lung injury are underway.[32]

Taken together, our studies reveal a specific *in vivo* role of p38α in OL development and myelination in the CNS. Opposite roles of p38α raise a therapeutic possibility of the p38α CKO

inhibition in myelin-deficiency diseases, such as MS and periventricular leukomalacia, but further studies are necessary to further define the underlying mechanisms. Nonetheless, the present study clearly identifies p38α as a key regulator of myelination and remyelination in the CNS.

Materials and Methods

Generation and genotyping of transgenic p38α^fl/fl and NG2/Plp^cre p38α^−/− (p38α CKO) mice. Generation of mice with floxed alleles of p38α (B6.129-Mapk14<tm1.2Otsu>) has been described previously.[18] NG2/Plp-cre recombinase-expressing mice as well as the recombination-reporter strain ROSA26-tdTomato (mT)-EGFP (mG) (Gt (ROSA) 26-Sortm4 (ACTB-tdTomato,-EGFP)Luo/J) were obtained from the Jackson Laboratory (Bar Harbor, ME, USA). Conditional NG2/Plp-specific p38α mice were generated using Cre/loxP recombination system by cross breeding NG2/Plp-Cre mice (FVB/N background) and p38α-floxed (p38α fl/fl) mice (C57BL/6 background). The NG2/Plp-Cre-positive heterozygous p38α mice were then backcrossed to p38α fl/fl mice to obtain mice homozygous for the p38α fl/fl with and without NG2/Plp-Cre. Mice were genotyped using tail-tip DNA by using the QIAamp DNA Mini Kit (Qiagen, Valencia, CA, USA). The genotypes of p38α fl/fl and p38α CKO mice were examined by analyzing two transgenic compositions in genomic DNA, including NG2/Plp-Cre and the presence of p38α-floxed alleles, using specific primers. All mice were maintained in accordance to the NIH guidelines for the Care and Use of Laboratory Animals. Experimental protocols used for this study were approved by the Institutional Animal Care and Use Committee at the University of California, Davis. The Cre-LoxP

recombination rate of NG2 Cre p38α CKO was ~ 57% and that of Plp Cre p38α CKO was ~ 63%.

Mixed glial cultures. Primary cultures of mixed glial cells were established from p38α CKO and p38α fl/fl (control) as previously reported.[33] In brief, the brains from P0 mice were removed and submerged in ice-cold Leibovitz L-15 medium. The Olfactory bulbs, cerebral cortex, and hindbrains were removed. Meninges with blood vessels and choroid plexus were carefully peeled off. Remaining tissues were cut into small pieces and digested using trypsin (0.0625% w/v) in HBSS for 20 min. Cells were dissociated by trituration and collected by centrifugation at $400 \times g$ for 5 min. Dissociated cells were suspended in MEM alpha containing FBS (10% v/v) and plated in a tissue culture dish. Cells were maintained in growth medium (GM), a mixture of N1 medium (high glucose DMEM supplemented with 6 mM l-glutamine, 10 ng/ml biotin, 5 μg/ml insulin, 50 μg/ml apo-transferrin, 30 nM sodium selenite, 20 nM progesterone and 100 μM putrescine) and B104 neuroblastoma-conditioned medium (7 : 3 mixture v/v). Media was changed daily, and the OPCs cultures were grown to confluency before purification.

Immunopanning for purification of primary OPCs. Purification of OPCs was performed using a two-step approach of negative and positive affinity selection using surface markers. Separate low-adhesion dishes (10 cm) were first coated overnight with secondary antibodies that bind rat IgG or mouse IgG. These plates with secondary antibodies were then incubated with the respective primary antibodies: either anti-Thy1 rat IgG (clone 30H12) or anti-NG2 mouse IgG at least 2 h before washing to remove unattached immunoglobulins. Mixed glial cultures were then trypsinized and resuspended in N1 medium containing 0.1% IgG-free BSA and plated on the anti-Thy1 IgG dish and incubated in a 37 °C, 5% CO$_2$ humidified environment for a 30-min negative selection. The non-adherent cell population from this dish was then removed and plated on the anti-NG2 IgG dish and incubated in a 37 °C, 5% CO$_2$ humidified environment for a 30-min positive selection. Adherent cells that represent primary OPCs were then collected by a rapid trypsinization using 0.5% Trypsin solution followed by buffered, purified soybean trypsin inhibitor (Gibco, Life Technologies, CA, USA, 500 μg/ml in HBSS). OPCs were then plated in poly-L lysine-coated plates with N1 medium supplemented with FGF2 (10 ng/ml) and PDGF-A (5 ng/ml).

Differentiation of OPCs to OLs. To induce *in vitro* differentiation of OPCs, the culture medium was switched from GM to OL differentiation medium (a 1 : 1 mixture of high glucose DMEM and Ham's F-12 supplemented with 4.5 mM L-glutamine, 10 ng/ml biotin, 12.5 μg/ml insulin, 50 μg/ml transferrin, 24 nM sodium selenite, 10 nM progesterone, 67 μM putrescine, 0.4 μg/ml 3,5,3′5′-tetraiodothyronine, 100 units/ml penicillin and 100 μg/ml streptomycin). Cultures were allowed to differentiate for 4 days, a time point at which $> 80\%$ of the control OLs from p38α fl/fl mice were positive for MBP.

RNA isolation and qPCR. The relative expression of transcription factors and markers associated with myelination in p38α CKO and p38α fl/fl OPCs and OLs were analyzed by qPCR. Total RNA was extracted from cultures of OPCs and OLs and was reverse-transcribed to cDNA using Multiscribe reverse transcriptase (Applied Biosystems, Foster City, CA, USA). Subsequent qPCR estimations were performed using Taqman primer-probe sets (Life Technologies) for Olig1 (Mm00497537_s1), Olig2 (Mm01210556_m1), Zfp488 (Mm02763085_s1), NG2 (Mm00507257_m1), CNPase (Mm01306640_m1), MPB (Mm01266402_m1) and PLP (Mm00456892_m1) in triplicate using a Lightcycler 480 (Roche Applied Science, Pleasanton, CA, USA). A relative efficiency plot was constructed for each gene to compare target and reference ΔCp values and ensure that the absolute slope of fit line is < 0.1.

Cuprizone-induced demyelination. CNS demyelination was induced by cuprizone in mice according to an established protocol.[34] Eight-week-old p38α CKO and p38α fl/fl male mice were fed either 0.2% cuprizone (w/w) (Lab Die, Richmond, IN, USA) or control pellet diets *ad libitum* for 5 weeks to induce demyelination. Food pellets were changed on alternate days, and body weight was recorded weekly. After 5 weeks, mice were returned to a regular diet to allow for remyelination.

Electron microscopy. Mice were perfused, and the brains were fixed overnight in Karnovsky's fixative (5% glutaraldehyde + 4% PFA in 0.08 M phosphate buffer), followed by postfixing in 2% osmium tetroxide in 0.1 M cacodylate buffer. Samples were subsequently dehydrated, placed in propylene oxide and then embedded in epon. Semi-thin (1 μm) sections were stained with toluidine blue to aid in orientation of white matter tracts. Ultrathin sections (70 nm) of the regions of interest were cut and collected on Formva-coated single slot copper grids. Sections were stained with uranyl acetate and lead citrate and examined in a Philips CM120 Electron Microscope (Hillsboro, OR, USA) at 80 kV. Low magnification images were taken to view the axon distributions, and high magnification images were obtained to show the myelin sheath layers for *g*-ratio calculation. Images were acquired via a high-resolution CCD camera (Gatan, Pleasanton, CA, USA) and processed in DigitalMicrograph (Gatan). Images were imported to Adobe Photoshop (San Jose, CA, USA) for adjusting the brightness and contrast and composing figures.

Immunoblotting. Western blotting analysis was carried out on total protein extracts from the whole brains of p38α CKO mice. Briefly, electrophoresis was performed in SDS-polyacrylamide gel, using 30 μg of proteins per lane. The following primary antibodies were used: mouse anti-MBP antibody (1 : 1000; Sternberger and Sternberger, Baltimore, MD, USA), rabbit polyclonal p38α antibody (1 : 200, Santa Cruz Biotechnology, Santa Cruz, CA, USA) and mouse anti-β-Actin monoclonal antibody (1 : 1000, Santa Cruz Biotechnology). Specific immunolabeling was obtained by using horseradish peroxidase-conjugated secondary antibodies, followed by the SuperSignalWest Pico chemiluminescence detection system (Pierce, Rockford, IL, USA).

Immunohistochemistry. Mice were deeply anesthetized with sodium pentobarbital (100 mg/kg, i.p.) and transcardially perfused with 0.9% NaCl in 0.1 M PBS, pH 7.4 followed by 4% PFA in 0.1 M PBS (pH 7.4). The brains were then dissected and postfixed in 4% PFA at 4 °C for 48 h. Brain tissues were cryoprotected, embedded in OCT and frozen. Then 40-μm-thick transverse cryosections were collected. Following primary antibodies were used: rabbit polyclonal, and mouse monoclonal anti-GFP antibodies (1 : 1000 dilution; Abcam, Cambridge, MA, USA) to identify EYFP, anti MBP antibody (1 : 500; Sternberger and Sternberger), and rabbit polyclonal anti-human Olig2 antibody (1 : 500; Abcam).

For the peroxidase immunohistochemistry, tissue sections were blocked with 10% normal goat serum and then incubated in 0.1 M PBS containing 0.1% Triton-X and the primary antibody for 16–18 h at 4 °C. Sections were then incubated with HRP-conjugated goat anti-rabbit or HRP-conjugated goat anti-mouse secondary antibodies (1 : 200; Jackson ImmunoResearch Laboratories, West Grove, PA, USA) for 2 h at room temperature. Diaminobenzidine (0.5 mg/ml) was used to visualize the reaction. Finally, sections were dehydrated and cover-slipped with Entellan mounting medium (BDH Chemicals, Toronto, ON, Canada).

Brain sections for fluorescent immunohistochemistry were blocked with 10% normal goat serum (Jackson ImmunoResearch Laboratories) and then incubated in PBS containing 0.1% Triton-X and the primary antibody overnight. Sections were then incubated for 2 h at room temperature in a mixture of Alexa 546-conjugated goat anti-rabbit IgG, Alexa 488-conjugated goat anti-mouse IgG and Alexa 643-conjugated goat anti-guinea pig IgG (Molecular Probes Inc., Eugene, OR, USA), at 1 : 2000 dilution. Sections were cover slipped in non-fluorescing mounting medium (Fluorsave Reagent, Calbiochem, La Jolla, CA, USA).

Data analysis. Photomicrographs of p38α fl/fl and p38α CKO brain sections were captured under identical setting, with a SPOT Cooled Color digital camera (Diagnostic Instruments Inc., Mawah, NJ, USA), mounted on a Zeiss microscope (Pleasanton, CA, USA) and assembled in Adobe Photoshop (version 9). For quantification of MBP staining intensity, ImageJ (Bethesda, MD, USA) was used. Selected areas (1 mm $\times$ 1 mm or 2 mm $\times$ 2 mm) were used to analyse statistical significances.

Electron microscopic photomicrographs were analyzed for myelination by calculation of the G (*g*) ratio (the ratio of axon circumference to myelin circumference). Briefly, high magnification images of myelinated axons were obtained and imported to the ImageJ software for measuring the diameter of the axons. The *g*-ratio was calculated as the diameter of the axon (*a*) divided by diameter of the myelinated axon caliber (*A*): *g*-ratio $= a/A$. Thus, the smaller the *g*-ratio is, the thicker is the myelin sheath layer. All of the data are represented as mean $\pm$ S.E.M. Each experimental group had at least eight mice. Statistical assessments were analyzed using ANOVA with *post-hoc* Tukey's test when multiple group comparisons were made and Student's *t*-test when two independent groups were compared. *P*-values of < 0.05 were considered significant.

Conflict of Interest

The authors declare no conflict of interest.

Author contributions
S-HC, VS, X-BL, HM and MH performed experiments and analyzed data; SB, JS, PJ, CC, FC and DEP provided critical input; WD directed the study; and S-HC and WD wrote the manuscript.

1. Gold R, Linington C, Lassmann H. Understanding pathogenesis and therapy of multiple sclerosis via animal models. 70 years of merits and culprits in experimental autoimmune encephalomyelitis research. *Brain* 2006; **129**: 1953–1971.

2. Khwaja O, Volpe JJ. Pathogenesis of cerebral white matter injury of prematurity. *Arch Dis Child Fetal Neonatal Ed* 2008; **93**: 153–161.

3. Deng W. Neurobiology of injury to the developing brain. *Nat Rev Neurol* 2010; **6**: 328–336.

4. Baumann N, Pham-Dinh D. Biology of oligodendrocyte and myelin in the mammalian central nervous system. *Physiol Rev* 2001; **81**: 871–927.

5. Miller RH. Regulation of oligodendrocyte development in the vertebrate CNS. *Prog Neurobiol* 2002; **67**: 451–467.

6. Emery B. Regulation of oligodendrocyte differentiation and myelination. *Science* 2010; **330**: 779–782.

7. Freshney NW, Rawlinson L, Guesdon F, Jones E, Cowley S, Hsuan J *et al.* Interleukin-1 activates a novel protein kinase cascade that results in the phosphorylation of Hsp27. *Cell* 1994; **78**: 1039–1049.

8. Zhang R, Murakami S, Coustry F, Wang Y, de Crombrugghe B. Constitutiveactivation of MKK6 in chondrocytes of transgenic mice inhibits proliferation and delays endochondral bone formation. *Proc Natl Acad Sci USA* 2006; **103**: 365–370.

9. Hui L, Bakiri L, Mairhorfer A, Schweifer N, Haslinger C, Kenner L *et al.* p38alpha suppresses normal and cancer cell proliferation by antagonizing the JNK-c-Jun pathway. *Nat Genet* 2007; **39**: 741–749.

10. Ventura JJ, Tenbaum S, Perdiguero E, Huth M, Guerra C, Barbacid M *et al.* p38alpha MAP kinase is essential in lung stem and progenitor cell proliferation and differentiation. *Nat Genet* 2007; **39**: 750–758.

11. Fragoso G, Robertson J, Athlan E, Tam E, Almazan G, Mushynski WE. Inhibition of p38 mitogen-activated protein kinase interferes with cell shape changes and gene expression associated with Schwann cell myelination. *Exp Neurol* 2003; **183**: 34–46.

12. Fragoso G, Haines JD, Roberston J, Pedraza L, Mushynski WE, Almazan G. p38 mitogen-activated protein kinase is required for central nervous system myelination. *Glia* 2007; **55**: 1531–1541.

13. Bhat NR, Zhang P, Mohanty SB. p38 MAP kinase regulation of oligodendrocyte differentiation with CREB as a potential target. *Neurochem Res* 2007; **32**: 293–302.

14. Hamanoue M, Sato K, Takamatsu K. Inhibition of p38 mitogenactivated protein kinase-induced apoptosis in cultured mature oligodendrocytes using SB202190 and SB203580. *Neurochem Int* 2007; **51**: 16–24.

15. Hossain S, de la Cruz-Morcillo MA, Sanchez-Prieto R, Almazan G. Mitogen-activated protein kinase p38 regulates Krox-20 to direct Schwann cell differentiation and peripheral myelination. *Glia* 2012; **60**: 1130–1144.

16. Yang DP, Kim J, Syed N, Tung YJ, Bhaskaran A, Mindos T *et al.* p38 MAPK activation promotes denervated Schwann cell phenotype and functions as a negative regulator of Schwann cell differentiation and myelination. *J Neurosci* 2012; **32**: 7158–7168.

17. Baron W, Metz B, Bansal R, Hoekstra D, de Vries H. PDGF and FGF-2 signaling in oligodendrocyte progenitor cells: regulation of proliferation and differentiation by multiple intracellular signaling pathways. *Mol Cell Neurosci* 2000; **15**: 314–329.

18. Nishida KO, Yamaguchi S, Hirotani S, Hikoso Y, Higuchi T, Watanabe T *et al.* p38alpha mitogen-activated protein kinase plays a critical role in cardiomyocyte survival but not in cardiac hypertrophic growth in response to pressure overload. *Mol Cell Biol* 2004; **24**: 10611–10620.

19. Zhou Q, Wang S, Anderson DJ. Identification of a novel family of oligodendrocyte lineage-specific basic helix-loop-helix transcription factors. *Neuron* 2000; **25**: 331–343.

20. Takebayashi H, Nabeshima Y, Yoshida S, Chisaka O, Ikenaka K, Nabeshima Y. The basic helix-loop-helix factor olig2 is essential for the development of motoneuron and oligodendrocyte lineages. *Curr Biol* 2002; **12**: 1157–1163.

21. Howng SY, Avila RL, Emery B, Traka M, Lin W, Watkins T *et al.* ZFP191 is required by oligodendrocytes for CNS myelination. *Genes Dev* 2010; **24**: 301–311.

22. Soundarapandian MM, Selvaraj V, Lo U, Golub MS, Feldman DH, Pleasure DE *et al.* Zfp488 promotes oligodendrocyte differentiation of neural progenitor cells in adult mice after cuprizone-induced demyelination. *Sci Rep* 2011; **1**: 2.

23. Chung SH, Guo F, Jiang P, Pleasure E, Deng W. Olig2/Plp progenitor cells give rise to Bergmann glia in the cerebellum. *Cell Death and Dis* 2013; **4**: e546.

24. Cui QL, Fang J, Kennedy TE, Almazan G, Antel JP. Role of p38MAPK in S1P receptor-mediated differentiation of human oligodendrocyte progenitors. *Glia* 2014; **62**: 1361–1375.

25. Godl K, Wissing J, Kurtenbach A, Habenberger P, Blencke S, Gutbrod H *et al.* An efficient proteomics method to identify the cellular targets of protein kinase inhibitors. *Proc Natl Acad Sci USA* 2003; **100**: 15434–15439.

26. Fabian MA, Biggs WH, Treiber DK, Atteridge CE, Azimioara MD, Benedetti MG *et al.* A small molecule–kinase interaction map for clinical kinase inhibitors. *Nat Biotechnol* 2005; **23**: 329–336.

27. Lluis F, Perdiguero E, Nebreda AR, Muñoz-Cánoves P. Regulation of skeletal muscle gene expression by p38 MAP kinases. *Trends Cell Biol* 2006; **16**: 36–44.

28. Weider M, Küspert M, Bischof M, Vogl MR, Hornig J, Loy K *et al.* Chromatin-remodeling factor Brg1 is required for Schwann cell differentiation and myelination. *Dev Cell* 2012; **23**: 193–201.

29. Li ZY, Yang J, Gao X, Lu JY, Zhang Y, Wang K *et al.* Sequential recruitment of PCAF and BRG1 contributes to myogenin activation in 12-O-tetradecanoylphorbol-13-acetate-induced early differentiation of rhabdomyosarcoma-derived cells. *J Biol Chem* 2007; **282**: 18872–18878.

30. Bachstetter AD, Van Eldik LJ. The p38 MAP kinase family as regulators of proinflammatory cytokine production in degenerative diseases of the CNS. *Aging Dis* 2010; **1**: 199–211.

31. Namiki K, Matsunaga H, Yoshioka K, Tanaka K, Murata K, Ishida J *et al.* Mechanism for p38α-mediated experimental autoimmune encephalomyelitis. *J Biol Chem* 2012; **287**: 24228–24238.

32. Gaestel M, Kotlyarov A, Kracht M. Targeting innate immunity protein kinase signalling in inflammation. *Nat Rev Drug Discov* 2009; **8**: 480–499.

33. Horiuchi M, Itoh A, Pleasure D, Ozato K, Itoh T. Cooperative contributions of interferon regulatory factor 1 (IRF1) and IRF8 to interferon-gamma-mediated cytotoxic effects on oligodendroglial progenitor cells. *J Neuroinflammation* 2011; **8**: 8.

34. Franco-Pons N, Torrente M, Colomina MT, Vilella E. Behavioral deficits in the cuprizone-induced murine model of demyelination/remyelination. *Toxicol Lett* 2007; **169**: 205–213.